

AquaGSat – A Sun Pointing Picosatellite Powered by a Regenerative Fuel Cell

Thomas Lowery, Kyle Ottinger

Texas A&M University – College Station, TX

Advisor: Dr. K. T. Alfried

Introduction

A unique opportunity of low-cost access to space in is being offered to many educational institutions and commercial interests around the world. The Cubesat program offers launch opportunities for pico-satellites (<1kg) which can be built for a reachable price range, thus extended the access to space out further into the public grasp. The current cubesat projects offer up to 200 grams of payload to be for small low-earth-orbit (LEO) experiments. Along with the increasing trend in small spacecraft, alternate forms of power are being developed. Such as the unitized regenerative fuel cell (URFC). A URFC extracts the energy from the formation of H₂O and utilizes it as power. The URFC has the ability to then reverse the process inputting the power necessary to break down the H₂O into H₂ and O₂ and storing the products. Thus, applied to space applications URFC serves as a non-hazards, cheap, and infinitely renewable energy source. AquaGSat will utilize this access to low-earth-orbit (LEO) by providing a platform for a small URFC and other experiments of similar power needs.

This report details the preliminary design of AquaGSat “Water EnerGy” Satellite. The AquaGSat was designed with a modular vision of being able to implement similar experimental payloads that share power and attitude control requirements. Design drivers for AquaGSat are: innovation, maximize energy per volume ratio, utilization of existing technology, and simplicity. The basic shape and composition of the external shell of the spacecraft is provided by the *P-POD Payload Planners Guide*. P-POD will eject its cubesat load at a certain location in orbit (600 km to 800 km). Once safely away the cubesats will activate themselves and begin their mission. To accomplish AquaGSat’s mission, it is a three-axis stabilized sun-pointing satellite, because of its large power needs.

The sections that follow consider the design and analysis that were performed. Including URFC, Mission Design, P-POD requirements, Thermal, Vibration and Structural Analysis, and Attitude

Determination and Control Model and Simulation results, Power and Communications subsystems.

1. URFC

A unitized regenerative fuel cell is water-based technology for space applications, generically called “Water Rocket”, which is the collective name for an integrated set of technologies that offer new options for spacecraft propulsion, power, energy storage, and structure. “Water-based technology” refers to the use of a water/gaseous hydrogen (gH₂)/gaseous oxygen (gO₂) cycle for propulsion, energy storage, and other applications.¹ The URFC technology is not yet available in this size so all data is linearly scaled down from much larger URFC sizes.

A normal fuel cell usually stores chemical reactants hydrogen and oxygen and directly converts them into electricity. The by product is water to be expelled or used somewhere else. A process known as electrolysis allows recycling of this water for use as a storage system.² With current electrochemical technology, a “static feed” electrolyzer, based on proton exchange membrane (PEM) technology can accept water at low pressure (several psig) and generate gasses at much higher pressure (up to 2000 psi). Electrolyzer and fuel cell functions can be combined into a single reversible electrochemical stack, called a unitized regenerative fuel cell (URFC).² It is AquaGSat’s goal to use a miniature version of the current URFC as its only power supply during the eclipse phase of orbit. A conceptual overview is shown in Fig. 1.1

1.1 Modes

There are two modes the URFC operates under, charge and discharge modes, see Figure 1.1.2a. Charge refers to the process by which H₂O (at 10’s of kPa) is fed into the cell by means of the PEM, there being electrolyzed, consuming energy to form H₂ and O₂. This H₂ and O₂ are then separated inside the cell and sent into their respective tanks at around 14 MPa.

Discharge occurs when the URFC is stack is reversed in process and H₂ and O₂ are fed into the cell to be combined together to H₂O. The energy emitted in this reaction is then harnessed by the fuel cell and used to run the satellite during eclipse or any other time that the satellite is not being completely powered by its solar cells.

1.2 Sizing the URFC

After researching the many cubesats currently being built the average weight set aside for scientific experiments is around 200 g. Therefore, the size for the payload must be kept under 200 grams so that it does not dominate other vital subsystems, both in mass and center of gravity (c.g.). Figure 1.1.2b, from LLNL, displays a linear trend in possible URFC sizes. For the purpose of this study, the slope was determined and the average input power our cubesat could supply was used to determine the estimated size of the URFC.

$$M_{URFC} = 0.0133 * P_{INPUT} \quad \text{Eq. 1-2-1}$$

From Eq. 1-2-1, and using an average power input from the solar panels of 4.6 Watts the size of the URFC was determined to be 61.2 g.

1.3 Initial On Orbit Setup

Since the location in orbit will not be known at the time of deployment the URFC will have to be prepared to immediately produce enough power to support the satellite. The amount of the H_2O electrolyzed in an hour was determined from linearly extrapolating from a list of LLNL/Hamilton Sundstrand Design of Static Feed Electrolyzers. A value of importance is the net electrolysis that occurs at 120°F. The trend is linear in nature and emulates that of the input power size. Therefore, scaling down the lowest figure of 2.8 g H_2O /hr to a mere 0.33 g H_2O /hr and using 48 minutes cycles, or roughly half an orbit, we obtain a figure of 0.53 g H_2O /orbit.

The density of water is 1 g/cc, so using the stoichiometric relationship the amount of water needed theoretically is 0.18g/cycle. But determining leakage and efficiency in the URFC and tanks is the point of the experiment so a specific amount of H_2O , H_2 and O_2 will be supplied in order to keep power output to the communications and command subsystem a continuous 2 Watts. The exact amount of "excess" must be determined by assuming a full discharge cycle of H_2 and O_2 needed to make it around to charge cycle. So a baseline of 0.16 g O_2 and 0.02 g H_2 must be stored. But there are also the efficiency and leakage to consider. So we have decided that we will arbitrarily set our maximum H_2O weight is set to 50 g.

1.4 Storage Tanks

H_2 and O_2 storage tank size will be dictated by the pressure and temperature during charge and

discharge. For this project, size of specific tanks will not be detailed only estimated based on simple principles.

The ideal gas law is employed to find the volume based on this pressure and operating temperature around the URFC.

The cost in mass of storing pressurized water is high. Instead an expulsion bladder that functions at low pressure can be employed.

1.5 URFC Realization

The size of AquaGSat's URFC is ten times smaller than any URFC currently in existence. An example of smaller technology would be this micro-sized fuel cell for cell phones developed by Fraunhofer Institute for Solar Energy Systems ISE.

'The scale for this application is confirmed to be outside the bounds that were considered for "Applications of Water Refuelable Spacecraft". Scaling to such small dimensions will be non-linear and a challenge that carries significant technical and financial risks. The specific energy advantage of URFC energy storage has not yet been proven at such small scale', Fred Mitlitsky.

Although, the data regarding the URFC power output and size is non-existent it serves as a useful exercise for the design of this pico-satellite.

2. Mission Design

Even though the orbit is predetermined by Cal Poly several factors were left to the designers discretion. The P-POD2 system may be launched aboard the OSP Space Launch Vehicle, and hard-mounted to the JAWSAT satellite as its primary payload. The launch vector of the CubeSats with respect to Earth and launch vehicle will not be unknown at the time of deployment, and all clients must accept this fact at time of CubeSat installation into the Deployer (P-POD).¹

2.1 Mission Requirements

The period and revolutions per day numbers were be used in sizing the spacecraft's communication, ADCS, and payload systems. The data rate is controlled by time in view, which is ultimately determined by period, this is key in sizing the antenna and flight processor. Since the spacecraft is sun-pointing the amount of torque needed to turn the spacecraft will be determined by the basic orbital parameters and is dealt with in the ADCS simulation. Using this

information the amount of H₂ and O₂ the URFC must be able to electrolyze during the eclipse to support the operations of the other subsystems was determined.

2.2 Lifetime Analysis

The purpose of the mission is to test the lifetime of the payload experiment so the lifetime is as long as it can operate.

One of the stipulations in the P-POD payload planners guide is that the mission designer show proof of safe spacecraft deorbit. But, considering the fact that we employ no ΔV so there will be no possibility of orbit transfer, also our mass and materials are such that they will safely burn during reentry.

2.3 Mission Summary

In summary, mission success would be defined as the acquisition of a vital fuel cell information transmitted over the course of an extended period. In order to achieve this objective the satellite must sun-point at all times and transmit during the appropriate time frame over the ground station. This mission is unique not only in its experiment but in its power generation and in solar array deployment. Much work needs to be completed before a CDR, the areas of work would include: complete structural, thermal, vibrational analysis, communications, and power system breakdown.

3. P-POD Integration Notes

Although P-POD's method is sound and cost effective several restrictions are imposed¹. Some of the more important restrictions of the P-POD Payload Planners are as follows:

- Temperature extremes: -40°C to 65°C
- Maximum Force during Launch: 15g's

Several analysis were performed with these restrictions in mind specifically; structural loading and vibration, and thermal analysis.

There are several topics to consider for the integration of AquaGSat into the P-POD device. First, the coarse sun sensor, to be discussed later must be maximum of 6.5 mm off the surface of the top panel. The H₂O in the storage tank must be able to unfreeze within one daylight half-orbit. The spring-loaded hinges must be designed in such a way so that the extreme temperatures do not effect its performance in orbit.

4. AquaGSat Configuration

AquaGSat's configuration internally is mainly the standard shelf design. The URFC, 3-axis magnetometer, and communications equipment are all supported by 1.12 mm thick shelving. What is unique about this cubesat is it's ability to deploy four sides thus effectively increasing the solar array area five fold. Some issues and concerns will be discussed in the following sections.

4.1 External Configuration Goals, Issues, and Concerns

The major goal of AquaGSat's unique configuration is the increase in solar array capacity. Other cubesats have had deployable solar arrays but none so ambitious as AquaGSat. The goal is obviously to generate the most power possible but also to gather this power in the simplest way imaginable. A 3-D view of the deployed sides is shown in Figure 1.1.1.

4.2 Component Placement

The main drive in the placement of the component was to place the c.g. of the satellite as close to the physical center as possible. Also of concern is to place the heavy magnetometer away from the magnetorquers so that they do not interfere with operation.

4.3 Preliminary Mass, C.G., and Inertia Estimates

The volume of the basic shape of a cubesat was calculated from the schematic provided in *The Payload Planner's Guide*. Using the density of aluminum the weight was found to be 242.66 g or 24.2% of the satellites dry weight.

The center of gravity (c.g.) of the shell was then calculated using Eq. 4-3-1.

$$(m_1 + m_2 + \dots)g_{cg} = m_1 g x_1 + m_2 g x_2 + \dots$$

Eq. 4-3-1

There are two modes for the center of gravity, one before deployment of the sides and then with the sides deployed. The only mode of importance for this study is that of the deployed mode because that is the configuration where all magnetic torquing will be performed. Thus the inertial matrix of the satellite will be transformed due to the change in the c.g. caused by deploying the solar panels. Upon further analysis, using ProE, the inertial matrix does not change significantly from a symmetric matrix (Table 4.3).

4.4 Deployment of the Solar Panels

Deployment is accomplished by designing the side panels to fold out upon being released from P-POD using spring loaded hinges triggered by the pressure release on the kill switches that occurs when the cubesat leaves the P-POD shaft. The spring loaded hinges will simply like vision glasses hinges. For purposes of this discussion the springs will be modeled as aluminum cylinders of length 8.3 cm and diameter 0.3 cm.

4.5 Future Work

The majority of the work for the configuration will be to determine how everything will be attached. Also, the design of these spring loaded hinges will be of key importance for post-PDR.

5. Thermal Control

In order to design a thermal control system, one must know the given thermal parameters that all components must lay within as well as the environment of the satellite. The following section details the preliminary design process of the thermal control system.

5.1 Thermal Requirements

From the temperature ranges of the inner components of AquaGSat, we can determine the acceptable limitations for temperature aboard the satellite. The controlling factor of the lower bound temperature will be the URFC (Unitized Regenerative Fuel Cell), which cannot drop below 0 °C without the water in the storage tank freezing. The upper bound limitation will be the electronic components, which can remain suitable for reliable use while the temperature is below 50 °C. Thus leaving the internal operating temperature of the satellite between 0-50 °C.

5.2 Thermal Environment and Operational Factors

There are several environmental factors that affect the thermal environment including but not limited to: operations, seasonal variation, and aging of paints and coating.⁶

Seasonal variation effects the solar flux experienced by the satellite. This value can vary from 1,326 W/m² to 1,418 W/m² depending on the season.

The aging of paints and coating is known as degradation effects. This is primarily the result of UV radiation.³ These degradation effects are asymptotic in nature but can still be quite drastic. Depending on the time duration of the mission, in our case as long as we can possibly ascertain

data, these degradation effects must become an integral part of thermal analysis.

Several operational factors must be included into the analysis of the thermal control. The amount of power dissipated by the inner working components is a notable factor. This dissipated power can significantly raise the working temperature of the satellite. Other operational factors that influence the temperature are the attitude and altitude of the satellite.³ These elements effect the levels of exposure to radiation.

5.3 Spherical Analysis

In order to determine a rough feasibility for thermal control a spherical satellite analysis is used. For this analysis we assume there is no uniform energy dissipation over the surface of the sphere and there is no electrical generation on the spherical surface.³ Several different surfaces were analyzed in our design process.

With all other variables assumed or given, determining the values of the absorptivity and emissivity were now required to proceed with thermal calculations. By modifying what material or coating was on the outside of our satellite we are effectively able to change the temperature ranges on the inside. An iterative approach was used to help determine the ideal values for absorptivity and emissivity. They were found to be 0.2 and 0.44 respectively. After researching thermal properties of a variety of materials, we found Teflon fluorinated ethylene propylene with vacuum deposited Aluminum (FEPAL) with a 0.5-mm thickness has an absorptivity and emissivity of 0.14 and 0.4 respectively.⁴ This presents a temperature range of 9 °C to 38 °C. This material can be found from Sheldahl, standard item number: 146431. Falling well within our bounds this material will be used as external coating on our picosatellite.

5.4 Results

We have established an allowable working range for temperature and through spherical analysis demonstrated that a Type A Teflon X Vacuum deposited Aluminum with a 0.5-mm thickness will allow our satellite to operate within the determined range.. Thus we will leave the thermal control completely passive with adjustments to the satellite's exterior as our only means of temperature control.

5.5 Thermal Summary

Although temperature analysis was carried out on the satellite, much more extensive calculations are required to verify that all components remain in acceptable bounds. A computer simulation of the heating and cooling through eclipse and sun phases coupled with a thermal finite element analysis of all applicable satellite components is still required. Only after that will we know without a shadow of a doubt if it is feasible to control the temperature of the satellite through completely passive means.

6. Attitude Determination and Control System

In designing the attitude determination and control subsystem (ADCS) our goal was to achieve a three-axis control devoted to maintaining solar panels alignment with the sun for highest efficiency of power.

6.1 Control System Selection

To help us achieve our goals there are four components of our ADCS subsystem: a magnetometer, a homemade coarse sun sensor, three magnetorquers, and a central processing unit (CPU).

We are using a three axis magnetometer from Billingsley Magnetics (Model # - TFM100G2-S). It is advantageous not only by being lightweight, 100g, but it also fits within the dimensions of our picosatellite, 3.51 x 3.23 x 8.26 cm.

The next component in our ADCS is a homemade sun sensor. The sun sensor works on the principle of power differentiation. The reading from each panel of the pyramid is used to determine pointing direction. Therefore all three panels have maximum readings when the satellite is perfectly aligned, or normal to the sun.

In order to physically control the satellite we will be using three magnetorquers, modified from off the counter model from ITHACO Space Systems, Inc (Catalog number: TR1UPN). Each will use the Earth's magnetic field and electrical current through the torquer to create magnetic dipole that results in torque on the vehicle. This torque can be used to stabilize tumbling spacecraft, control the spin of spinning spacecraft or manage the momentum in 3-axis stabilized spacecraft.

6.2 Disturbance Environment

There are four main external torques on the satellite. Gravity gradient effects, which are

based on the fact that elongated objects in a gravity field tend to align their longitudinal axis through the Earth's center. Magnetic field torques which stem from the fact that the Earth's magnetic field is not a constant value but varies through the orbit. Solar radiation, which also varies with orbit and time, it is constant for solar-oriented vehicles. The last of the four is aerodynamic torque, which is related to the drag experienced by the satellite due to the amount of Earth's atmosphere that it is encountering.⁶ Gravity gradient and magnetic torque are much stronger in our instance, but if the solar array deployment were less symmetric, solar radiation and aerodynamic torques would increase considerably in significance.³

6.3 Sun Pointing Control System

In order to increase the efficiency of the solar arrays our satellite must remain sun pointing. Unlike setting up a simulation for earth pointing satellites, a sun pointing satellite must include the movement of the earth about the sun. Another reason for the intricacy of reference frames is that we are sun pointing while using the Earth's magnetic field for control. These added stipulations create a complex arrangement of coordinate systems and coordinate transformations between them.

To better understand the simulation at this point we will expound upon the coordinate systems.

The body frame, B, is fixed in the body with B1 being the yaw axis, B2 the roll axis, and B3 the pitch axis. In aircraft terminology the yaw is up, the roll axis is out the front and the pitch axis is out the left wing.

In the sun frame, S, S1 is directed from the sun to the vernal equinox, S2 is in the ecliptic in the direction of motion of the Earth, and S3 is perpendicular to the Earth orbit plane.

The inertial frame, I, is Earth centered with the I1 axis pointing towards the first point of Aries, it is parallel to S1. The I3 axis is along the Earth polar axis and I2 is perpendicular in the equatorial plane.

The Earth frame, E, rotates with the Earth. It coincides with the S frame at Vernal equinox.

The orbit frame, O, moves with the satellite with O1 out the radius vector, O2 in the orbit plane and O3 perpendicular to the orbit plane.

The last reference frame is the most important. This is the frame that points at the sun, the D frame. This will be the frame of reference from which we reference pitch, roll, and yaw. Its origin coincides with the B and O frames. The D3 axis points towards the sun and the plane

formed by the D1 and D3 axes to go through the center of the Earth. The D2 axis is in the orbit plane. To obtain D from O, you must rotate O1 by an amount ψ and then about the new O2 by an amount ϕ .⁵

After assigning the frames of reference we needed to write the equations of motion in the body frame, B, with the roll, pitch, and yaw angles defined relative to the D frame. Once all coordinate transformations have been carried out and we have solved the Euler equations, we are ready to impose a control law. This is seen in Equation 6.1

$$M_3 = -K_1 B_1 \phi + K_2 B_2 \Psi - K_3 B_1 \phi + K_4 B_2 \Psi$$

Eq. 6.1

Where M is the magnetic dipole about the B3 axis, the K values are the gains, and the B values are that of the Earth's magnetic field, in the bodyframe. The gains are given by Equations 6.2-6.5.

$$K_1 = \frac{\omega^2 J_{22}}{B_1^2}$$

Eq. 6.2

$$K_2 = \frac{\omega^2 J_{11}}{B_2^2}$$

Eq. 6.3

$$K_3 = \frac{2\zeta\omega^2 J_{22}}{B_1^2}$$

Eq. 6.4

$$K_4 = \frac{2\zeta\omega^2 J_{11}}{B_2^2}$$

Eq. 6.5

Where $\omega = 0.1$ and $\zeta = 1$.

For simulation purposes lets assume that we are in a magnetic polar orbit. The resulting Earth's magnetic field can be modeled as seen in Equations 6.6-6.9.

$$\bar{B}_0 = B_0 \left(\frac{R_e}{r} \right)^3$$

Eq. 6.6

$$\bar{B}_1^2 = 4\bar{B}_0^2$$

Eq. 6.7

$$\bar{B}_2^2 = \bar{B}_0^2$$

Eq. 6.8

$$\bar{B}_3^2 = 0$$

Eq. 6.9

The AquaGSat on-orbit control system will use the pitch magnet for control and yaw. Rotation will be allowed along the pitch axis. All three magnetorquers will be required to procure initial acquisition.

6.4 Control System Performance

The purpose of running a computer simulation of the control system in this case is to validate two essential values. We first want to prove that the satellite can be recovered from some given displacement to ideal, which is sun pointing. Furthermore we would like to prove that the magnetorquers will provide the necessary force to keep the satellite controlled.

In analyzing the recovery time for the AquaGSat, we shall take a look at the Euler rates and Euler angles as a function of time. Our analysis represents an initial offset of 25° in the psi direction. We can see from Figure 6.1.1 that at about 5400 seconds all Euler angles have been brought to near zero values. This determines that it will take 9 minutes to bring the satellite back to normal with the sun. We can see the same representation from figure 6.1.2, the plot of Euler rates.

We next want to evaluate if the torque provided by the magnetorquers has a great enough force to control the satellite's attitude. Figure 6.1.3 was plotted using the same initial offset as before. You will see that the torque never exceeds 1.5×10^{-8} N-m². The torque available from one magnetorquer, assuming the Earth's magnetic field to be 4.5×10^{-5} tesla is 5.22×10^{-5} N-m². This value will be more then required for control.

6.5 Control Summary

More intensive programming will be needed in order to turn the control algorithm on and off through sun and eclipse phases of orbit. It would also be beneficial to do a greater detailed analysis of disturbance torques and their effect on the satellite.

11. Power

The Power Subsystem is given the responsibility of generating, storing, conditioning, and distributing the power to operate the spacecraft. There are several different methods used to accomplish this task and most spacecraft power systems are unique in their designs. The AquaGSat is no different, and in fact presents a

few unique design parameters that must be incorporated into the power subsystem.

11.1 Solar Cell Array

The AquaGSat will use traditional solar cell arrays to generate power during sunlight periods. It will do this by incorporating Gallium Arsenide cells since they achieve higher efficiencies, can operate at higher temperatures, and exhibit greater radiation tolerances. The solar array design will incorporate ten solar cells that will be deployed on five faces on the spacecraft. The properties for the Emcore GaAs cells are displayed in Table 11.1.

The faces will deploy via hinges to create a large array that will face the sun at all times in order to maximize power generation. The faces will be deployed as in Figure 1.1.

Using the GaAs parameters the maximum power generation can be calculated with the following equation.

$$P_{\max} = Q * n * l \times w * e * (1 - \alpha)$$

Eq. 11-1-1

Using these equations with 10 solar cells the maximum power that can be achieved is 7.8 Watts. Emcore offers custom made solar cells so as to maximize the available surface area on the exterior of the satellite. The five faces that will be used on the satellite combine for an available surface area of 419 cm². If custom made solar cells are used then the number of cells could be as high as 14, which in turn will produce approximately 11 Watts. Which cells to use depends on the accuracy of the ADCS control system

11.2 Power Budget

The average values for the electrical components were found from their respective providers, Table 11.2. Summing the average values results in the amount of power that the URFC must produce during eclipse. Which directly translates into the amount power needed to input during the charge or daylight phase. This value is found by assuming an efficiency of 34%-50% for the URFC².

For worst case the maximum power is computed for the components, thus finding the maximum URFC power or the power that the satellite must have at all times during the daylight phase.

Using Eq. 11.-2-1, you find the maximum angle from the sun, 26.5°, that the satellite can deviate and still generate the correct power.

$$P_{\text{result}} = P_{\text{generated}} \cos(\theta)$$

Eq. 11-2-1

Where θ is the sun incidence angle. P_{result} is 6.98 W and P_{gen} is 7.8 W. This translates directly into the error for the sun pointing magnetic control law discussed previously. Thus using the custom fit cut will only increase this angle and reduce torquing.

All of the components that operate the satellite operate at the same voltage but not the same current levels. Table 11.2 listing all of the components and their projected voltage and current levels are shown in Table 11.2.

12. Conclusions

The feasibility of building AquaGSat has yet to be determined. URFC technology has not yet progressed to the point which micro-fuel cells are readily available. The design of AquaGSat was to provide a housing for a pico-experiment which requires greater power then that available to a normal picosatellite. By inducing the satellite to remain sun pointing the power generation greatly increases while complicating the design of the attitude control system. While we believe we have overcome these complexities, many simulations are required to ensure constant available power to the payload during sun phases.

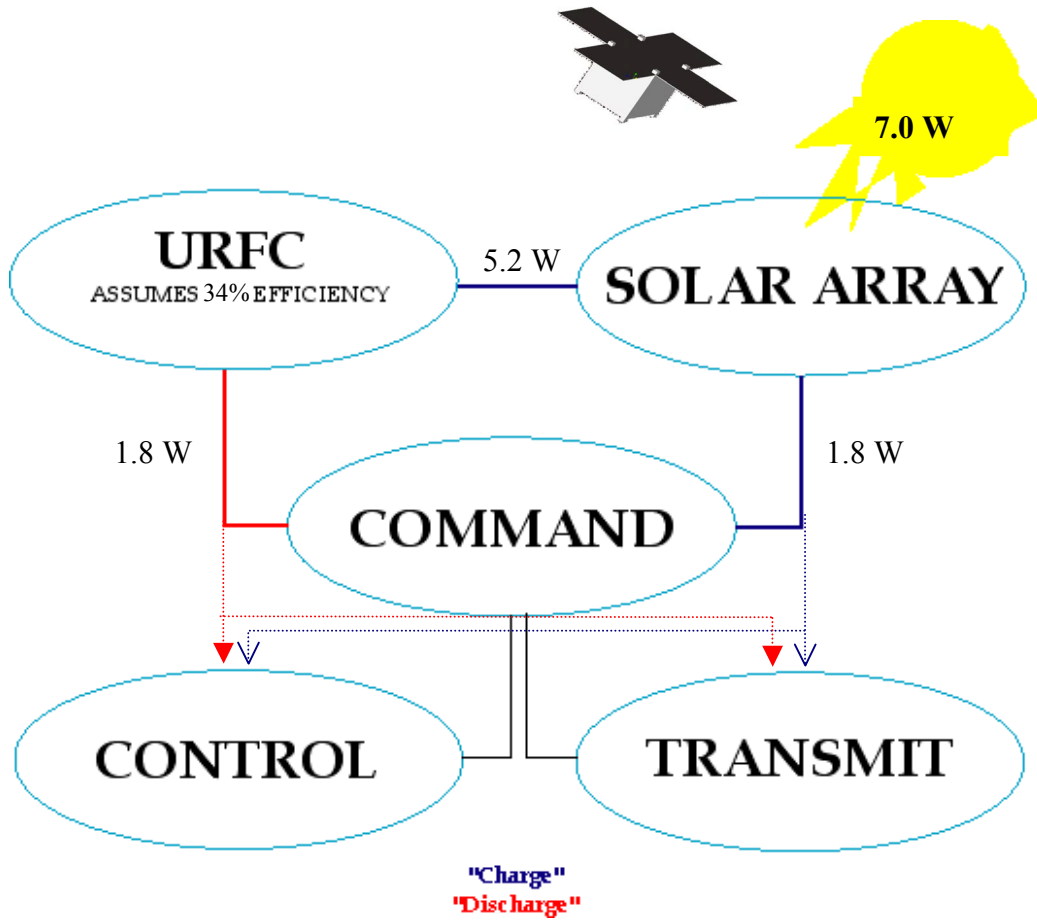


Figure 1.1.1. Conceptual Overview of Subsystems

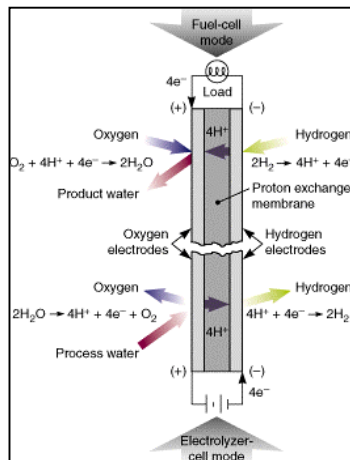


Figure 1.1. Operational Modes of URFC⁸

AquaGSat: A Sun Pointing Picosatellite Powered by a RFC
Texas A&M University

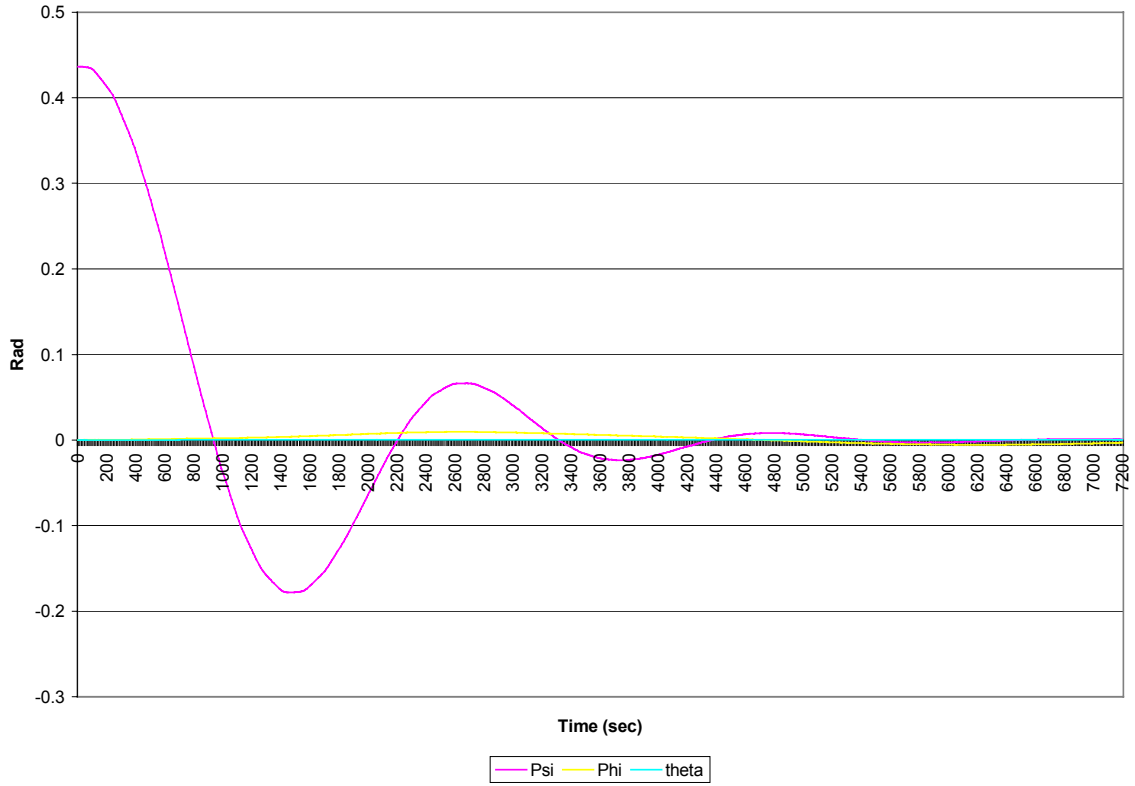


Figure 6.1.1 Euler Angles vs. Time [psi0=25deg,phi=0,theta=0,rates=0]

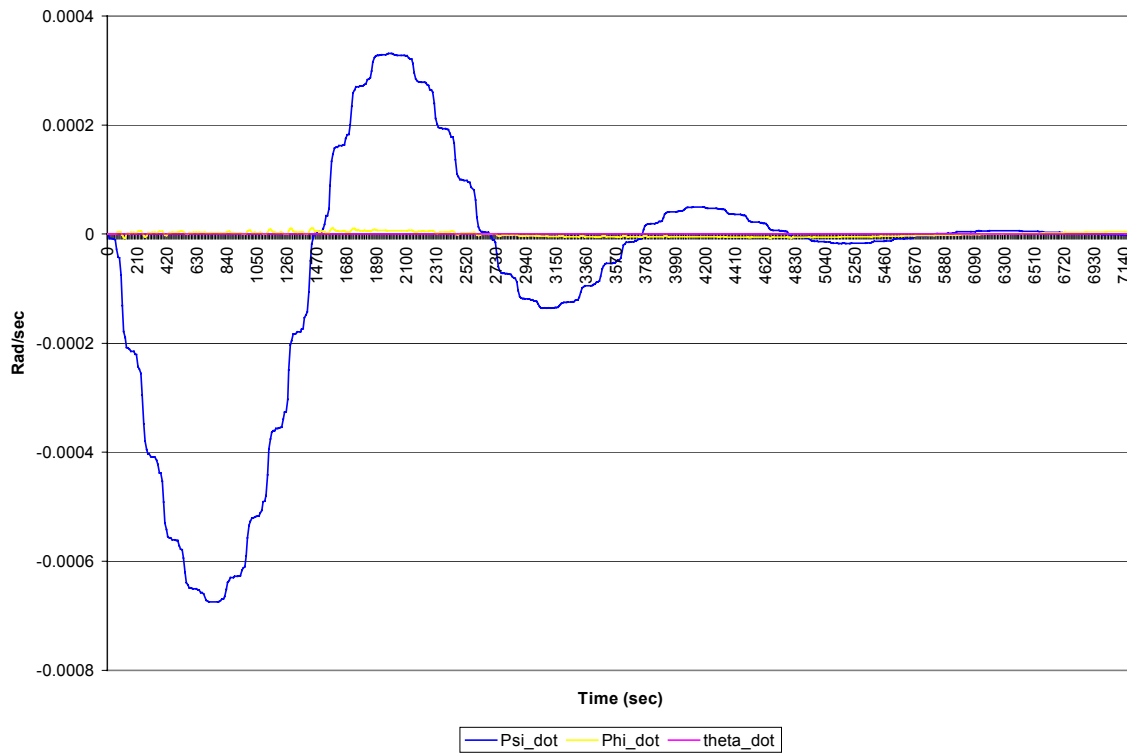


Figure 6.1.2 Euler Rates vs. Time [psi0=25deg,phi=0,theta=0,rates=0]

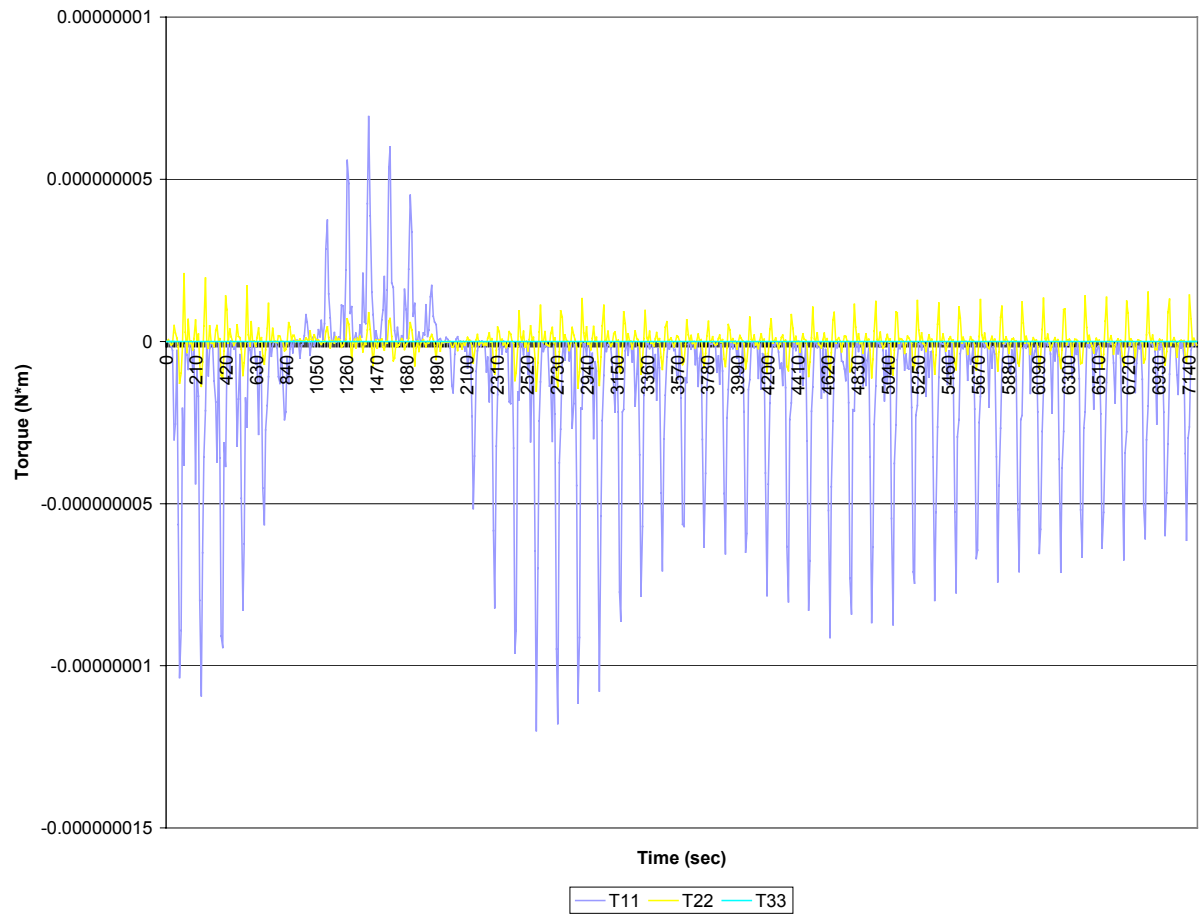


Figure 6.1.3 Torques vs. Time [psi0=25deg,phi=0,theta=0,rates=0]

<i>Quantity</i>	<i>Description</i>
<i>Supporting Surface Area</i>	419 cm**2
<i>Cell Type</i>	GaAs
<i>Cell Dimension</i>	7.6 x 3.7 cm
<i>Number of cells (n)</i>	10
<i>mass of each</i>	2.4 g
<i>Total Mass</i>	37.44 g
<i>Operating Temp</i>	50 C
<i>Efficiency(e)</i>	23% at 28 deg. C
<i>Temp Effect (α)</i>	11 % per deg. C
<i>Solar Intensity(Q)</i>	0.135 W/cm**2
<i>Output</i>	7.8
<i>Custom Fit</i>	10.9

Table 11.1. Solar Array Design

<i>Subsystem</i>	<i>Component</i>	<i>Current*</i>	<i>Avg. Power</i>	<i>Max. Power</i>
<i>Payload</i>	URFC	0.8343	4.1714	5.17
<i>TT&C</i>	H8/3337F S-Mask Model + mem	0.0300	0.1500	0.20
	transmitter/receiver (MC13145,6)	0.0420	0.2100	0.25
	modulation/demodulation with the MSP430	0.0100	0.0500	0.06
	antenna	0.2000	1.0000	1.00
<i>ADCS</i>	TFM100G2-S Three-Axis Magnetometer	0.0100	0.0500	0.10
	torqueroil similar to that of TR1UPN, Ithaco	0.0000	0.0000	0.20
<i>Total</i>		1.1263	5.6314	6.98
<i>Power Mode</i>	<i>Component</i>	<i>Total Current*</i>	<i>Worst case Power</i>	

Table 11.2. Power Budget

References:

- ¹. R. Connolly, *The P-POD Planners Guide*, Revision C, June 5, 2000
- ². F. Mitlitsky, "Applications of Water Refuelable Spacecraft," DARPA/TTO, January5, 2000.
- ³. W.J. Larson and J. R. Wertz, *Space Mission Analysis and Design*, Microcosm Inc., Torrance, CA and Kluwer Academic Publishers, Neterlands, 1992.
- ⁴. D.G. Gilmore, *Satellite Thermal Control Handbook*, The Aerospace Corporation Press, El Segundo, California, 1994
- ⁵. K. T. Alfriend, *ACS Simulation*, 2001
- ⁶. J. Juang, *Space Mission Design AERO 485 Notes*, Spring 2001
- ⁷. SMAD, Support Software
- ⁸. www.fuelcells.org